International Journal for Modern Trends in Science and Technology
Volume 12, Issue 03, pages 512-520.
ISSN: 2455-3778 online
Available online at: http://www.ijmtst.com/vol12issue03.html
DOI: https://doi.org/10.5281/zenodo.20566856

Potential Removal of Malachite Green Dye from Wastewater Using Natural Soda Feldspar as an Adsorbent: Kinetic, Equilibrium, and Thermodynamic Studies

Madhusudhana Reddy. Mule[1*] | K.V. Ramesh[2] | G. V. S. Sarma[2] | K. Sarath Chandra[3]

[1]*Department of Chemical Engineering, RGUKT Nuzvid, Nuzvid-521202, India.*
[2]*Department of Chemical Engineering, Andhra University College of Engineering (A), Visakhapatnam-530003, India.*
[3]*SCRACS(OFC) Pvt. Ltd., Buchireddypalem-524305, India.*

To Cite this Article
Madhusudhana Reddy. Mule, K.V. Ramesh, G. V. S. Sarma & K Sarath Chandra (2026). Potential Removal of Malachite Green Dye from Wastewater Using Natural Soda Feldspar as an Adsorbent: Kinetic, Equilibrium, and Thermodynamic Studies. International Journal for Modern Trends in Science and Technology, 12(03), 512-520. https://doi.org/10.5281/zenodo.20566856

Article Info
Received: 24 February 2026; Revised: 21 March 2026; Accepted: 25 March 2026.

KEYWORDS
Soda feldspar; Malachite Green; Adsorption; Wastewater treatment; Adsorption kinetics; Adsorption isotherms; Thermodynamics.

ABSTRACT

This study investigated the adsorption of Malachite Green (MG), a toxic cationic dye, onto natural soda feldspar as a low-cost mineral adsorbent. The effects of contact time, solution pH, initial dye concentration, adsorbent dosage, and temperature were evaluated to optimize the adsorption process. Maximum dye removal was achieved at pH 8, a contact time of 90 min, an adsorbent dosage of 15 g L^{-1}, and higher temperatures. Kinetic studies revealed that the adsorption process follows the pseudo-second-order model, indicating strong interactions between MG molecules and the active sites of soda feldspar. Equilibrium data were best described by the Redlich–Peterson and Langmuir isotherm models, suggesting a combination of homogeneous and heterogeneous adsorption with a maximum adsorption capacity of 34.49 mg g^{-1}. Thermodynamic parameters confirmed that the adsorption process is spontaneous and endothermic. Thus, the results demonstrate that soda feldspar is an effective and economical adsorbent for the removal of Malachite Green from aqueous media, offering a promising option for sustainable wastewater treatment.

INTRODUCTION

Rapid industrial growth has led to the discharge of large quantities of dye-containing wastewater into the environment, creating serious concerns for water quality and aquatic ecosystems[1],[2]. Among various synthetic dyes, malachite green (MG) is a cationic triphenylmethane dye extensively used in textile dyeing, leather processing, paper manufacturing, aquaculture, and as an

antifungal agent. Despite its widespread applications, MG is considered as a hazardous pollutant because of its persistence in the environment and its carcinogenic, mutagenic, teratogenic, and genotoxic effects on living organisms[3]-[6].

A variety of treatment methods, including coagulation–flocculation, membrane filtration, advanced oxidation, photocatalytic degradation, electrochemical treatment, and biological processes, have been explored for the removal of dye pollutants from wastewater[7]. However, many of these techniques are associated with high operational costs, complex procedures, or the generation of secondary pollutants. In contrast, adsorption has emerged as one of the most efficient and practical approaches due to its simplicity, high removal efficiency, operational flexibility, and ability to utilize low-cost adsorbents without producing harmful by-products[8].

Many adsorbents, including graphene-based materials[2], clays[4], activated carbons[5], biochars[10], and chitosan composites[11], have been successfully employed for the removal of malachite green from aqueous solutions. Despite their promising adsorption performance, many of these materials require chemical modification, thermal activation, or complex preparation procedures, which can increase production costs and hinder their large-scale application.

Natural aluminosilicate minerals such as clays, zeolites, and feldspars have emerged as promising low-cost adsorbents because of their abundance, environmental compatibility, and ion-exchange properties[8],[12],[13]. Feldspars, the most abundant rock-forming minerals, possess negatively charged aluminosilicate frameworks and exchangeable cations that facilitate pollutant adsorption through electrostatic attraction, ion exchange, and surface complexation mechanisms[14],[15].

Previous studies have demonstrated the effectiveness of feldspar minerals for the adsorption of various pollutants, including methylene blue, ferric ions, and arsenate, highlighting the important role of surface aluminosilicate and aluminol sites in contaminant removal [12],[15],[16]. Therefore, due to its abundance, low cost, chemical stability, and negatively charged aluminosilicate framework, soda feldspar ($NaAlSi_3O_8$) is a promising adsorbent for cationic dye removal. However, its application for malachite green adsorption has received limited attention. Therefore, the present study evaluates the potential of natural soda feldspar for malachite green removal from aqueous solutions by investigating the effects of operational parameters and analyzing the adsorption kinetics, equilibrium, and thermodynamic behavior of the process.

2. MATERIALS AND METHODS

Malachite Green ($C_{52}H_{54}N_4O_{12}$), a triphenylmethane dye (molecular weight = 927), was procured from M/s SDFCL, India. The molecular structure of the dye is shown in Fig. Powdered Soda Feldspar (NF) is a naturally available material procured from Andhra Pradesh, India. The powdered particles were sieved, and particles of size -140 mesh +170 mesh were collected, with an average size of 96.5 μm used in all the experimental studies. All reagents used in this investigation were of A.R. grade. Double-distilled water was used for preparing solutions throughout the study.

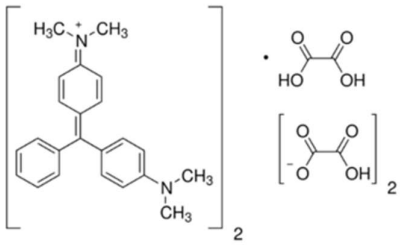

Fig. 1: Molecular structure of Malachite Green dye

All pH measurements were carried out with a digital pH meter, model WTH-10, M/s Wensar, India. The concentration of the dye solutions was estimated from absorbance readings recorded on a UV/VIS spectrophotometer (model CE7400, M/s Cecil, England) at 616 nm. The phase analysis studies were conducted on a Rigaku X-ray diffractometer (Japan), equipped with Cu-kα radiation (λ~1.54 ºA) , in the scan range (2θ) of 20º-50º. The morphological features were examined using scanning electron microscopy with energy-dispersive spectroscopy (FE-SEM, ZEISS Ultra 55 GEMINI, Germany).

Experimental studies were mainly conducted using batch techniques for obtaining rate and equilibrium data. The studies were carried out to examine the influence of contact time, solution pH, and adsorbent dosage at specified sample concentrations while maintaining constant temperature, particle size, and agitation speed. The operating parameter range is presented in Table 1. A specified quantity of adsorbent was placed in 250 mL volumetric flasks, each holding 50 mL of an MV adsorbate solution with a known concentration. The flasks were thereafter agitated intermittently to achieve adsorption

equilibrium. The resultant solution was subsequently centrifuged and analysed spectrophotometrically at 616 nm.

Table 1: Operating Parameters range in this study

Process Parameter	Parameter Range
Contact time (min)	0 – 120
Initial pH	2 – 10
Initial Concentration (mg/L)	25 – 250
Adsorbent dosage (g/L)	2 – 20
Temperature (°C)	40 – 60

The extent of adsorption was quantified in terms of percentage removal and adsorption capacity using the following equations (1) and (2).

$$Percentage\ removal(\%) = \frac{(C_o - C_t)}{C_o} \times 100 \ldots(1)$$

$$q_t = \frac{(C_o - C_t)V}{W} \ldots(2)$$

Duplicate experiments were carried out for all the operating variables studied, and only the average values were considered. The average deviation of duplicate results in the concentration units varied within ±1%.

3. RESULTS AND DISCUSSION

Characterization of Adsorbent material

The X-ray diffractograms of NF sample before and after adsorption of MG dye are showed in Fig. 2. It can be seen that the NF sample (cf. Fig. 2a) is majorly constituted with quartz (marked with ♦, JCPDS card no. 46-1045), microcline (marked with ■, JCPDS card no.19-0926), and albite (marked with ●, JCPDS card no. 09-0466) minerals. After adsorption of MG dye onto the NF, the NF-MG sample has shown nearly similar diffraction pattern (cf. Fig. 2b), as like pristine NF sample (cf. Fig. 2a). However, a sharp reduction in the peak intensity of mineral phases in NF-MG sample diffraction spectrum (cf. Fig. 2b) suggests that the MG dye molecules were entrapped on the rough surfaces and porous structure of NF[16]. But the existence of similar mineral phase assemblage in both NF and NF-MG samples clearly indicate the importance of microstructural features for understanding the MG dye adsorption mechanism by NF.

The scanning electron microscopy (SEM) images of pristine NF samples before adsorption are showed in Fig. 3. The bulk part of the NF sample exhibited a porous microstructure with random dense packing (cf. Fig. 3a). Here the densely packed tabular feldspar particles were randomly arranged and adjoined through a porous network in all parts of the sample NF microstructure. Such an adsorbent microstructure[13] is known to possess the interconnected porosity with a wide range of pore sizes (cf. Fig. 3b) and rough surfaces (cf. Fig. 3c) that work as active sites for dye adsorption. Similarly, the scanning electron microscopy (SEM) images of the NF-MG sample after adsorption of MG on NF are displayed in Fig. 4. A bulk portion of the NF-MG microstructure (cf. Fig. 4a) has exhibited a strong MG dye adsorption as a thin layer of coating throughout the active sites available for adsorption, as shown in Fig. 3. The pore filling phenomenon of MG dye adsorption is presented in Fig. 4b. Whereas the adsorption of MG dye onto the rough surface portions of the tabular feldspar particles can be evidenced from Fig. 4c. These observations are in consistent with the XRD results. EDS data of NF and NF-MG samples are displayed in Fig. 5. The coexistence of dominant peaks related to [Na], [Al], [Si], [O], with minor amounts of [K] in EDS spectrum of the NF sample (cf. Fig. 4a) confirms the chemical composition of soda feldspar. On the plus side, the EDS spectrum of NF-MG sample (cf. Fig. 5b) has exhibited the characteristic peaks of [C], [N], corresponding to the malachite green dye (C52H54N4O12) composition. A careful analysis of EDS spectra of both NF versus NF-MG validates the adsorption of MG dye on NF. Aluminosilicate minerals with lower Si/Al ratio are known to produce higher concentration of negatively charged aluminol (Al-OH) sites[17] that accelerates the adsorption of positively charged MG dye molecules through electrostatic interactions and hydrogen bonding[18]. Here feldspar (NF) belongs to aluminosilicate family. MG is a cationic dye. EDS data of pristine NF sample has shown Si/Al ratio of 4.1 (cf. Fig. 5a), which is significantly lower than the Si/Al ratio (~4.7) of NF-MG sample after adsorption (cf. Fig. 5b). This feature further confirms that chemisorption phenomenon is also involved in the removal of malachite green (MG) dye using soda feldspar (NF) as an adsorbent.

Effect of contact time

The influence of contact time on MG adsorption by NF was studied at two different initial concentrations of dye, i.e., 25 and 75 mg/L (Fig. 6). Initially, the adsorption rate

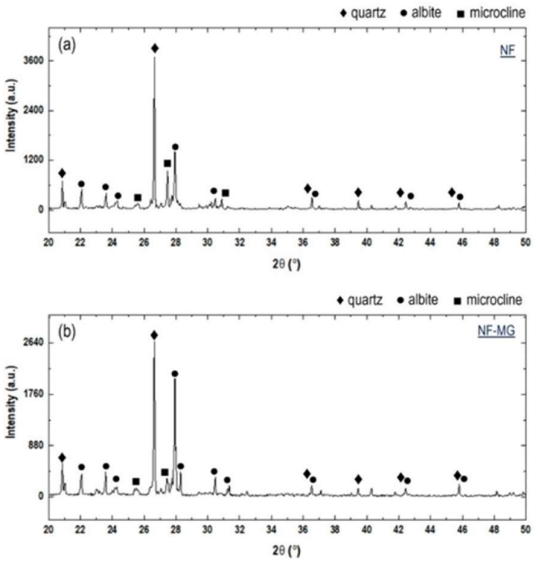

Fig. 2: X-ray diffraction patterns of (a) NF and (b) NF-MG samples.

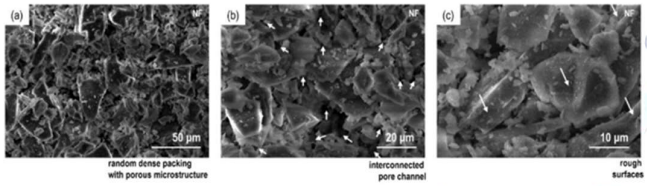

Fig. 3: Scanning electron micrographs of pristine soda feldspar (NF) samples before adsorption.

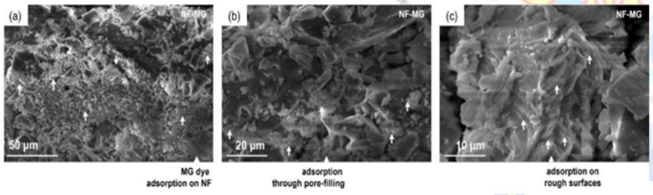

Fig. 4: Scanning electron micrographs of NF-MG samples after adsorption.

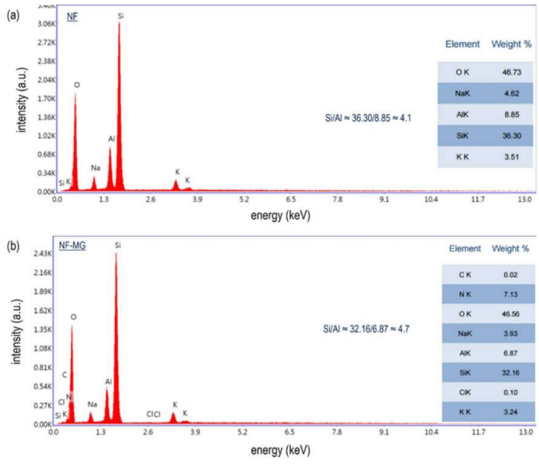

Fig. 5: SEM-EDS analysis of (a) NF and (b) NF-MG samples.

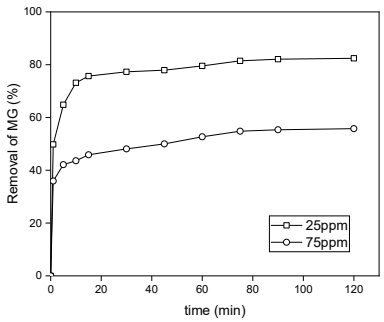

Fig. 6: Effect of contact time

was high because of the large number of accessible active sites on the surface of the adsorbent, and thereafter decreased with the occupation of these active sites. MG removal was 49.66% and 36.46% at 25 and 75 mg/L, respectively, in the first minute. Subsequently, the adsorption rate slowed down until equilibrium was reached. Equilibrium was achieved at 90 min for both concentrations, and this equilibrium time was used for the subsequent studies. The maximum dye removal efficiencies were 82.35% and 55.56% for 25 and 75 mg/L solutions, respectively, indicating that adsorption effectiveness declined with increasing initial dye concentration.

Effect of pH

The acid-base properties of functional groups on the adsorbent surface can be changed through pH adjustments, leading to ionization. This, in turn, enables the formation of electrostatic interactions between MG and NF, thus inducing the adsorption process. The effect of pH on the adsorption of MG at an initial dye concentration of 50 mg/L and 4 g/L adsorbent dosage is shown in the Fig. 7. This indicates that MG adsorption efficiency on the NF increases as pH increases from 2 to 9. Particularly, within the pH range of 6 to 9, adsorption efficiency is higher in this range. Based on the pH adsorption profile, a pH value of 8 is identified as an optimum condition, yielding a maximum adsorption efficiency of 76.86 percent; the decline in removal efficiency beyond pH 9 can be due to enhanced negative charge (OH-) of NF leads to electrostatic repulsion.

Effect of initial concentration

The effect of initial dye concentration on the adsorptive removal of MG by NF is shown in the Fig. 8. The experiment was carried out in the range of initial dye concentration, starting from 25 mg/L to 250 mg/L. The adsorption capacity 4.487 mg/g to 26.073 mg/g, as the initial dye

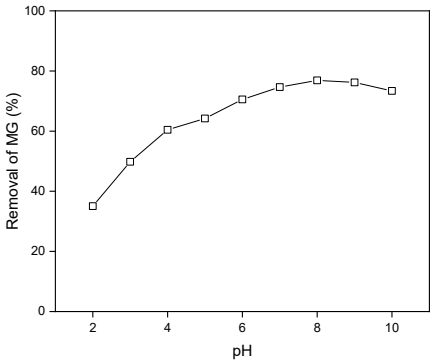

Fig. 7: Effect of pH

.

concentrations varied from 25 mg/L to 250 mg/L. Based on the profiles, it was observed that dye uptake increases while percentage removal decreases with an increase in initial concentrations of MG as the dosage was fixed at 4 g/L; at high initial dye concentrations, the number of dye molecules available for adsorption increases, leading to a higher amount of dye being adsorbed on to the NF surface, however, the percentage removal decreases because the adsorption capacity on the NF surface becomes saturated. The excess dye molecules remain in the solution.

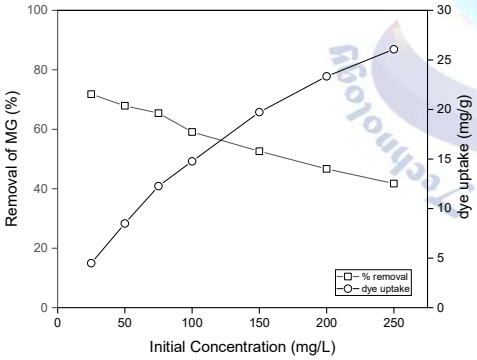

Fig. 8: Effect of initial concentration

Effect of adsorbent dosage

The impact of adsorbent dosage on the removal of MG dye was investigated by varying the amount of NF from 2 g/L to 20 g/L, and the other conditions were fixed at an initial concentration of 100 mg/L, solution pH, and room temperature. The results, as shown in the Fig. 9, revealed that the removal percentage of MG dye increased significantly from 15.55 percent to 88.65 percent as the adsorbent dosage was increased to 15 g/L and then negligible increase up to 89.12 percent with further increase in dosage up to 20 g/L. Hence, beyond the dosage of 15 g/L, the entire adsorbent surface may not be available due to the agglomeration of adsorbent particles, or the adsorbate concentration in the solution was insufficient to saturate the available binding sites. On the other hand, a decreasing trend was observed in the adsorption capacity, which decreased from 8.99 mg/g to 4.461 mg/g, indicating that the excess adsorbent dose led to agglomeration of the particles. This study suggested that the dosage of 15 g/L was optimum for the given conditions.

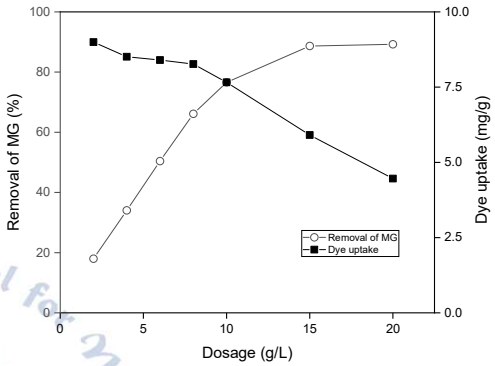

Fig. 9: Dosage effect

Effect of temperature

The adsorption studies revealed a positive correlation between temperature and adsorption capacity, with experiments conducted at 313K, 323K, and 333K yielding increasing adsorption capacities as shown in the Fig. 10. This trend tells that the adsorption process is endothermic; it adsorbs heat and is favored by higher temperatures. The observed enhancement in adsorption with rising temperature can be due to the increased kinetic energy of the dye molecules, which enhances their movement, enables them to collide more frequently with the adsorbent, and facilitates stronger interaction with the adsorbent.

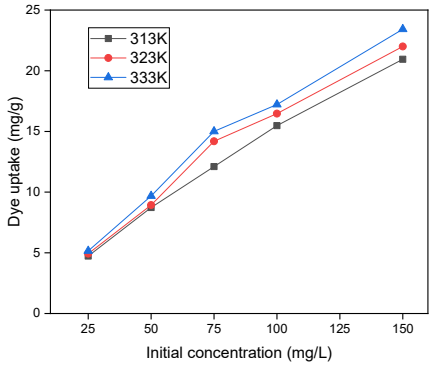

Fig. 10: Effect of temperature

Adsorption kinetics

Studying adsorption kinetics is essential for understanding how adsorption occurs. It shows how quickly adsorption occurs and how it changes over time. Two commonly used kinetic models, Pseudo-first-order and Pseudo-second-order, were applied to interpret the experimental data. The linear forms of these two models[9] are represented in equations (3) and (4).

Pseudo-first order model: $ln(q_e - q_t) = ln(q_e) - K_1 t$..(3)

Pseudo-second order model: $\frac{t}{q_t} = \frac{1}{K_2 q_e^2} + \frac{1}{q_e} t$..(4)

Linear fitting of the experimental data was performed at two different initial concentrations, as shown in Fig. 11 and Fig. 12. The results indicate that the Pseudo-second-order model accurately described the data, with R2 close to one. Conversely, as shown in Table 2, the Pseudo-first-order model provided a poorer fit, with a lower value. The Pseudo-second-order model accurately captured the MG adsorption behavior on NF, suggesting that electrostatic forces between the dye molecules and the adsorbent functional groups drive the adsorption process.

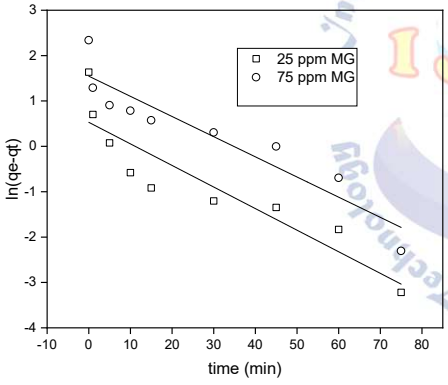

Fig. 11: Pseudo- first- order model linear fitting

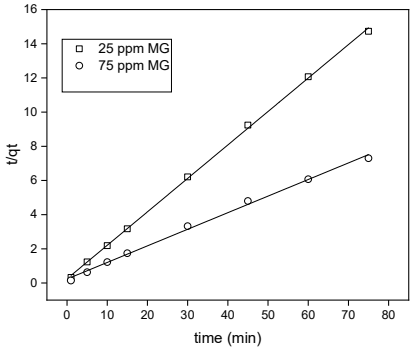

Fig. 12: Pseudo- second- order model linear fitting

Table 2: Kinetic parameters for the adsorption of MG onto NF

Parameter	**Values**	
Initial concentration of MG (mg/L)	25	75
Experimental q_e values (mg/g)	5.13	10.37
Pseudo-First order		
Rate constant K_1	0.05	0.04
Calculated q_e value (mg/g)	1.69	4.69
Correlation coefficient (R^2)	0.83	0.87
Pseudo-Second order		
Rate constant K_2	0.14	0.04
Calculated q_e value (mg/g)	5.11	10.23
Correlation coefficient (R^2)	0.99	0.99

Equilibrium studies

Adsorption isotherm analysis was performed using Langmuir, Freundlich, Temkin, Dubinin–Radushkevich, and Redlich–Peterson models[9],[19] to understand the interaction between malachite green (MG) and soda feldspar. Linear forms of all these models, as given in the equations (5) through (9), were used to fit the experimental data and determine the equilibrium parameters as tabulated in Table 3. Fig. 12 tells how well these models predict the equilibrium conditions. Among the tested models, the Redlich–Peterson isotherm provided the best fit ($R^2 = 0.99$), followed by the Langmuir model ($R^2 = 0.99$), indicating that MG adsorption occurs through a combination of homogeneous and heterogeneous surface interactions. This suggests that the soda feldspar surface contains both uniform and energetically diverse adsorption sites.

Langmuir Isotherm	$\frac{C_e}{q_e} = \frac{C_e}{q_m} + \frac{1}{K_L q_m}$ …(5)
Fruendlich Isotherm	$ln\, q_e = ln\, K_F + \frac{1}{n} ln\, C_e$ …(6)
Temkin Isotherm	$q_e = B(ln\, K_T) + B(ln\, C_e)$ …(7) $B = \frac{RT}{b_T}$
Dubinin–Radushkevich (D–R) Isotherm	$ln\, q_e = ln\, q_s - K_{DR}\varepsilon^2$ …(8) $\varepsilon = RTln(1 + \frac{1}{C_e})$
Redlich–Peterson Isotherm	$\ln\left(K_R \frac{C_e}{q_e} - 1\right) = ln\alpha + \beta ln\,(C_e)$ …(9)

The excellent agreement with the Langmuir model further indicates that MG molecules form a predominantly monolayer on the adsorbent surface. The maximum adsorption capacity predicted by the Langmuir model was 34.94 mg g^{-1}. Overall, the isotherm results reveal that the adsorption mechanism involves strong dye–surface interactions on well-defined active sites, together with

adsorption on heterogeneous regions of the mineral surface, contributing to the effective removal of MG by soda feldspar.

Table 3: Isotherm parameters for the adsorption of MG onto NF

Isotherm model	Parameters	Units	Value	R^2	Remarks
Langmuir	q_m	mg/g	34.49	0.99	Best fit
	K_L	L/mg	0.02		
Freundlich	K_F	(mg/g)/(mg/L)$^{(1/n)}$	1.65	0.98	good fit
	n	-	1.74		
Temkin	K_T	L/mg	0.21	0.98	good fit
	b_T	J/mol	346.42		
Dubinin-Radushkevich	K_{DR}	L/mg	1.4e-5	0.74	Bad fit
	q_s	mg/g	17.29		
Redlich-Peterson	K_R	L/mg	1.28	0.99	Best fit
	α	(L/mg) $^{\beta}$	0.28		
	β	-	0.60		

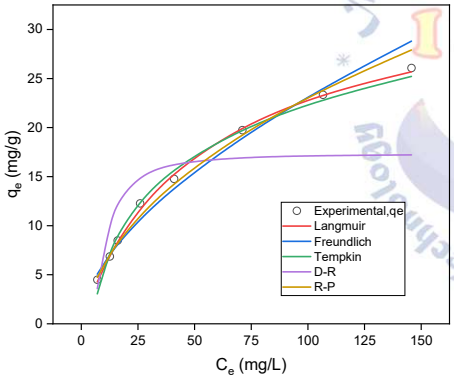

Fig. 12: Comparison of various adsorption isotherms

Adsorption thermodynamics

Thermodynamic analysis was carried out to evaluate the feasibility, spontaneity, and thermal nature of the adsorption process. The standard Gibbs free energy change (ΔG°) was calculated using the Langmuir equilibrium constant (KL) according to equation (10). The standard enthalpy change (ΔH°) and entropy change (ΔS°) were determined from the slope and intercept of the plot of ΔG° versus temperature (T), respectively following the equation (11) [5].

$$\Delta G^0 = -RT\, ln(K_L) \quad \ldots(10)$$

$$\Delta G^0 = \Delta H^0 - T\Delta S^0 \quad \ldots(11)$$

As illustrated in Fig. 13, the slope and intercept of the plot of ΔG against T were used to estimate the values of ΔH and ΔS of the adsorption of MG dye. Estimated thermodynamic parameters are provided in Table 4.

The adsorption of MG onto adsorbent NF was indicated to be possible and spontaneous thermodynamically by the negative free energy changes (ΔG). The fact that ΔH is positive further suggests that the adsorption process is endothermic. The change in entropy ΔS is also positive, which indicates the release of water (solvent) molecules from the adsorbent surface.

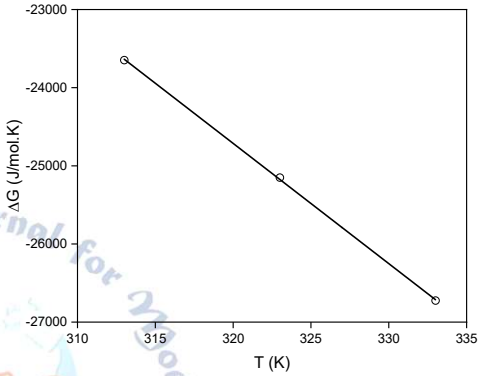

Fig. 13: Gibbs free energy change

Table 4: Thermodynamic parameters for the adsorption of MG onto NF

Temperature (K)	Langmuir Constant, K_L (L/mg)	ΔG (kJ/mol)	ΔH (kJ/mol)	ΔS (J/mol.K)
313	0.0242	-23.6472	24.531	153
323	0.0321	-25.1514		
333	0.0427	-26.7251		

4. CONCLUSION

The experimental findings demonstrate the suitability of soda feldspar as a natural, cost-effective adsorbent for the removal of Malachite Green from aqueous solutions. Adsorption efficiency was strongly influenced by operational parameters, with optimum performance observed at pH 8, 90 min contact time, 15 g L^{-1} adsorbent dosage, and elevated temperature. The adsorption process followed pseudo-second-order kinetics, indicating that dye uptake is controlled by interactions between MG molecules and the adsorbent surface's active sites. Analysis of isotherm models showed excellent agreement with the Redlich–Peterson and Langmuir models, suggesting that adsorption occurs through both homogeneous and heterogeneous surface sites, with a maximum adsorption

capacity of 34.49 mg g^{-1}. Thermodynamic studies revealed negative Gibbs free energy values along with positive enthalpy and entropy changes, confirming that the adsorption process is spontaneous, feasible, and endothermic. The combined results indicate that soda feldspar removes MG via monolayer adsorption on active mineral sites, along with adsorption on energetically diverse surface regions. Owing to its low cost, natural abundance, and good adsorption performance, soda feldspar has significant potential as a sustainable adsorbent for the treatment of dye-containing wastewater.

Nomenclature

Symbol	Abbreviation	Units
t	Time	min
V	Volume of solution	L
W	Mass of the adsorbent	g
C_e	Equilibrium concentration of adsorbate solution	mg/L
C_o	Initial concentration of adsorbate solution	mg/L
C_t	Concentration of adsorbate solution at any time	mg/L
q_e	Amount of adsorbate per unit mass of adsorbent at equilibrium	mg/g
q_m	Langmuir constant	mg/g
q_t	Amount of adsorbate per unit mass of adsorbent at time t	mg/g
K_F	Freundlich constant	L/mg
K_L	Langmuir constant	L/mg
K_{DR}	Mean free energy exchange	mol^2/kJ^2
K_T	Temkin isotherm equilibrium binding constant	L/mg
b_T	Temkin constant	J/mol
K_R	Redlich-Peterson constant	L/mg
E	Adsorption energy	kJ/mol
K_1	Pseudo-first-order rate constant	min^{-1}
K_2	Pseudo-second-order rate constant	$(mg/g)^{-1}$ min^{-1}
n	Freundlich heterogeneity factor	(-)
α	Redlich-Peterson constant	$(L/mg)^{\beta}$
β	Redlich-Peterson exponent	(-)
ε	Polanyi potential	kJ/mol
T	Temperature	K
ΔG	Change in Gibbs free energy	J/kmol
ΔH	Change in enthalpy	J/kmol
R	Ideal gas constant	J/mol·K
ΔS	Change in entropy	J/kmol

Conflict of interest statement

Authors declare that they do not have any conflict of interest.

References

[1] Agarwala R, Mulky L. Adsorption of dyes from wastewater: a comprehensive review. Chem Bio Eng Rev. 2023;10(3):326-335. DOI: https://doi.org/10.1002/cben.202200011

[2] Gupta K, Khatri OP. Reduced graphene oxide as an effective adsorbent for removal of malachite green dye: plausible adsorption pathways. J Colloid Interface Sci. 2017;501:11-21. DOI: https://doi.org/10.1016/j.jcis.2017.04.035

[3] Ahmad R, Kumar R. Adsorption studies of hazardous malachite green onto treated ginger waste. J Hazard Mater. 2010;91:1032-1038. DOI:https://doi:10.1016/j.jenvman.2009.12.016

[4] Arellano-Cárdenas S, López-Cortez S, Cornejo-Mazón M, Mares-Gutiérrez JC. Study of malachite green adsorption by organically modified clay using a batch method. Appl Surf Sci. 2013;280:74-78. DOI: https://doi.org/10.1016/j.apsusc.2013.04.097

[5] Nethaji S, Sivasamy A, Thennarasu G, Saravanan S. Adsorption of malachite green dye onto activated carbon derived from Borassus aethiopum flower biomass. J Hazard Mater. 2010;181(1-3):271-280. DOI: https://doi.org/10.1016/j.jhazmat.2010.05.008

[6] Sadiq AC, Rahim NY, Suah FBM. Adsorption and desorption of malachite green by using chitosan-deep eutectic solvents beads. Int J Biol Macromol. 2020;164:3965-3973. DOI: https://doi.org/10.1016/j.ijbiomac.2020.09.029

[7] Dastkhoon M, Ghaedi M, Asfaram A, Goudarzi A, Langroodi SM, Tyagi I, Agarwal S. Ultrasound assisted adsorption of malachite green dye onto ZnS:Cu-NP-AC: equilibrium isotherms and kinetic studies–response surface optimization. Sep Purif Technol. 2015;156(2):780-788. DOI: https://doi.org/10.1016/j.seppur.2015.11.001

[8] Sevim F, Lacin O, Ediz EF, Demir F. Adsorption capacity, isotherm, kinetic and thermodynamic studies on adsorption behaviour of malachite green onto natural red clay. Environ Prog Sustain Energy.2020;40(1):e13471. DOI: https://doi.org/10.1002/ep.13471

[9] Ahmad MA, Afandi NS, Adegoke KA, Bello OS. Optimization and batch studies on adsorption of malachite green dye using rambutan seed activated carbon. Desalin Water Treat. 2016;57(45):21487-21511. DOI: https://doi.org/10.1080/19443994.2015.1119744

[10] Vyavahare GD, Gurav RG, Jadhav PP, Patil RR, Aware CB, Jadhav JP. Response surface methodology optimization for sorption of malachite green dye on sugarcane bagasse biochar and evaluating the residual dye for phyto and cytogenotoxicity. Chemosphere. 2018;194:306-315. DOI:https://doi.org/10.1016/j.chemosphere.2017.11.180

[11] Muinde VM, Onyari JM, Wamalwa B, Wabomba JN. Adsorption of malachite green dye from aqueous solutions using mesoporous chitosan-zinc oxide composite material. Environ Chem Ecotoxicol. 2020;2:115-125. DOI: https://doi.org/10.1016/j.enceco.2020.07.005

[12] Al-Anber MA. Adsorption of ferric ions onto natural feldspar: kinetic modeling and adsorption isotherm. Int J Environ Sci Technol. 2015;12(1):139-150. DOI: https://doi.org/10.1007/s13762-013-0410-1

[13] GVS Sarma, K Sudha Rani, K. Sarath Chandra, Bonige Kishore Babu & KV Ramesh, Potential removal of phenol using modified laterite adsorbent, Indian Journal of Biochemistry and Biophysics. 2020; 57(5), pp. 613-619. DOI: https://doi.org/10.56042/ijbb.v57i5.37928

[14] Larsen E, Johannessen NE, Kowalczuk PB, Kleiv RA. Selective flotation of K-feldspar from Na-feldspar in alkaline environment. Miner Eng. 2019;142:105928. DOI: https://doi.org/10.1016/j.mineng.2019.105928

[15] Yazdani MR, Tuutijärvi T, Bhatnagar A, Vahala R. Adsorptive removal of arsenic(V) from aqueous phase by feldspars: kinetics, mechanism, and thermodynamic aspects of adsorption. J Mol Liq. 2016;214:149-156. DOI: https://doi.org/10.1016/j.molliq.2015.12.002

[16] Tian Y, Liu P, Wang X, Lin H. Adsorption of malachite green from aqueous solutions onto ordered mesoporous carbons. Chem Eng J.2011; 171(3): 1263–1269. DOI: https://doi.org/10.1016/j.cej.2011.05.040.

[17] Chutia P, Kato S, Kojima T, Satokawa S. Arsenic adsorption from aqueous solution on synthetic zeolites. J Hazard Mater. 2019; 162(1):440–447. DOI: https://doi.org/10.1016/j.jhazmat.2008.05.061.

[18] Mahinroosta M, Moattari RM, Allahverdi A, Ghadir P. Malachite green dye removal with aluminosilicate nanopowder from aluminum dross and silicomanganese slag. Circular Economy. 2024; 3(3):100100. DOI: https://doi.org/10.1016/j.cec.2024.100100

[19] Anirudhan TS, Ramachandran M. Adsorptive removal of basic dyes from aqueous solutions by surfactant modified bentonite clay (organoclay): Kinetic and competitive adsorption isotherm. Process Saf Environ Prot. 2015; 95:215-225. DOI: https://doi.org/10.1016/j.psep.2015.03.003